Received: Added at production | Revised: Added at production | Accepted: Added at production
DOI: xxx/xxxx

COMMUNICATION

Xylopyranose ring-opening by single and double proton transfers under pyrolysis conditions

Jacopo Lupi[1,2,3] | **Bernardo Ballotta**[1,2] | **Leandro Ayarde-Henríquez**[1,2] | **Stephen Dooley**[1,2]

[1]School of Physics, Trinity College Dublin, Dublin 2, Ireland
[2]AMBER, Advance Materials and BioEngineering Research Centre, Dublin 2, Ireland
[3]Current affiliation: CNR-ICCOM, Consiglio Nazionale delle Ricerche, via Giuseppe Moruzzi 1 Pisa I-56124, Italy

Correspondence
Corresponding authors Jacopo Lupi and Bernardo Ballotta
Email: jacopo.lupi@cnr.it;
Email: bernardo.ballotta@tcd.ie

Abstract

This study unveils a new transition state (TS) leading to the acyclic product via synchronous double proton transfer by automatedly exploring the potential energy surface of β-D-xylopyranose under pyrolysis conditions. Quantum chemistry methods with multi-path canonical variational transition state theory, show that the standard activation enthalpy of the new TS (46.4 kcal mol^{-1}) is 1.5 kcal mol^{-1} lower than that of the well-established channel; however, the latter's rate constant (4.36×10^{-2}-9.96×10^{1} s^{-1}) is higher in the 673.15-873.15 K pyrolytic interval by a factor of 5-8. This gap narrows to a factor of 2 within 320-400 K, signifying that the new TS can potentially impact the acyclic product production in this low-temperature range. This is particularly relevant for β-D-xylopyranose trimers, as the interior unit bears different substituents at the C1 and C3 positions.

KEYWORDS
Hemicellulose, automated reaction mechanism discovery, gas-phase thermochemistry, multi-path canonical variational transition state theory (MP-VTST), multi-structural torsional method (MS-T)

In recent decades, β-D-xylopyranose (hereafter termed xylopyranose), the hemicellulose building block, has received significant attention. Indeed, recent studies have focused on elucidating its structure, pyrolytic reactivity, and the effects of its functionalization Ayarde-Henríquez et al. (2024), Ballotta et al. (2024). It is widely accepted in the literature that the predominant reaction pathway for xylopyranose thermal decomposition is the ring-opening reaction Hu et al. (2019). This process is a concerted reaction involving a hydrogen transfer from the anomeric hydroxyl group to the ring oxygen, forming open-chain D-xylose (hereafter termed xylose). Recent high-level electronic structure calculations and kinetic analysis have determined a standard activation enthalpy of 43.5 kcal mol^{-1} for this elementary step, resulting in a faster reaction rate compared to other potential initial reaction channels Lupi et al. (2024). To the best of the authors' knowledge, no alternative ring-opening transition states (TSs) have been proposed until now. Utilizing state-of-the-art automated reaction discovery codes (AutoMeKin, Martínez-Núñez et al. (2021)), we report a new reaction pathway leading to the formation of xylose, which undergoes a synchronous 2-H proton transfer. This newly identified mechanism is illustrated in Fig. 1, alongside the well-known 1-H proton transfer mechanism. Canonical rate constants for both reactions are also computed employing multi-path variational transition state theory (MP-VTST).

METHODS

Discovery of Xylopyranose Ring-Opening Reaction Mechanisms

Reaction pathways for xylopyranose ring-opening processes were generated using the AutoMeKin program Martínez-Núñez (2015ab), Martínez-Núñez et al. (2021), which is designed for automated reaction mechanism discovery. AutoMeKin employs methodologies rooted in graph theory, reactive molecular dynamics, and electronic structure calculations to fully explore potential energy surfaces (PESs), thereby facilitating the identification of potential reaction mechanisms.

The dynamic simulations required to obtain the initial TS structures were conducted with the semi-empirical PM7 method Stewart (2013) as implemented in the MOPAC package Stewart (2016). For these simulations, ten trajectories per iteration were calculated over 100 total iterations. To screen and avoid redundant structures resulting from intermediate fragmentation, we applied specific criteria: the smallest accepted imaginary frequency was set at 100 cm^{-1} (keyword `imagmin`), to account for torsional TSs, and the lowest eigenvalue of

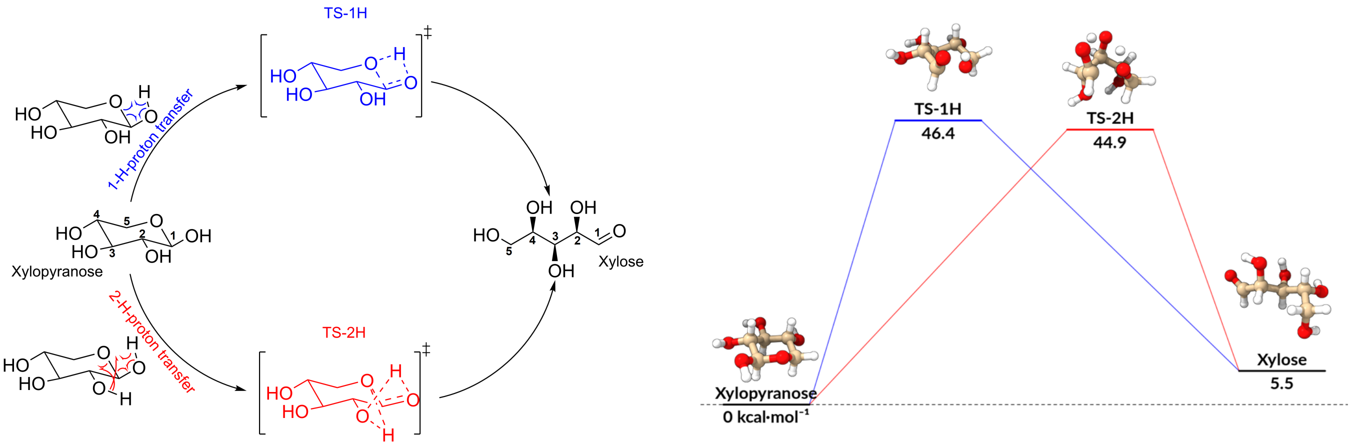

FIGURE 1 In the left panel: Single (TS-1H) and double (TS-2H) proton transfer mechanisms lead to the ring-opening of xylopyranose. In the right panel: The ring-opening barriers of both pathways, showing that the standard activation enthalpy of the new TS-2H lies 1.5 kcal mol^{-1} below. The new pathway is in red, and the known channel is in blue.

the Laplacian was set to 0.1 (keyword `eigLmax`). Additional screening parameters, such as MAPE max and BAPE max, were set to 0.002 and 1.5, respectively, to compare descriptors characterizing the structures obtained from the molecular dynamics simulations. Further details on these parameters are provided in ref. Martínez-Núñez et al. (2021).

Subsequently, optimized geometries and zero-point corrected electronic energies for all PES's critical points, such as reactants, TSs, intermediates, and products, were determined using the revDSD-PBEP86 Kozuch and Martin (2011)-D3(BJ) Grimme et al. (2011) double-hybrid functional in combination with the jun-cc-pVTZ basis set Papajak et al. (2011), hereafter referred to as rDSD. Optimized Cartesian coordinates are reported in the Supporting Information (SI).

The characterization of such structures along the reaction pathways as either minima (reactants, intermediates, products) or saddle points (TSs) was achieved through diagonalization of analytical rDSD Hessians. Moreover, intrinsic reaction coordinates (IRCs) Fukui (1981) were traced starting from the identified TSs to characterize the elementary steps further and ensure the TSs connect the correct reactant and product. All DFT calculations were performed using Gaussian16 Frisch et al. (2016).

The extensive and complex reaction networks generated by AutoMeKin were analyzed using the AMK tool Garay-Ruiz et al. (2022), which facilitates the visualization of molecular structures, vibrational normal modes, and potential energy profiles of the investigated reaction mechanisms. Through this approach, we identified possible reaction pathways leading to xylopyranose ring-opening and characterized the critical points governing these processes.

Energy Refinement

The electronic energies were refined by using the DLPNO-CCSD(T) level of theory (Riplinger et al. (2013)), with the F12 explicit correlation correction, on top of revDSD geometries. This method was selected due to its proven ability to deliver results that closely approximate those of the canonical CCSD(T) approach while significantly reducing the computational cost. The tightPNO cutoff setting was used to increase the accuracy of the localized pair natural orbital (PNO) approach, ensuring reliable results for the most complex systems. The choice of the cc-pVTZ-F12 basis set, Peterson and Dunning (2002), provides an optimal balance between computational efficiency and accuracy, particularly when combined with explicitly correlated methods. All DLPNO calculations were performed using the ORCA quantum chemistry program Neese (2022). The outcomes show that the new TS-2H is energetically favorable as its standard activation enthalpy is approximately 1.5 kcal mol^{-1} lower than the one characterizing the single proton transfer. See Fig. 1, right panel.

Kinetics

Within VTST's framework, computing rate constants involves critical aspects, including variational effects and torsional anharmonicity, especially for systems with multiple conformers (or structures) of reactants and TSs. The program `Pilgrim` Ferro-Costas et al. (2020) enables the detailed computation of thermal rate constants considering these factors by gauging MP-VTST and treating the torsional anharmonicity via subroutines implemented in the `MSTor` program Chen et al. (2023).

For a reaction proceeding from a reactant to a product through a TS, the canonical rate constant $k(T)$ at the absolute temperature T is given by the Eyring equation within the framework of conventional transition state theory (TST):

$$k(T) = \kappa(T)\frac{k_B T}{h}\frac{Q^{\ddagger}(T)}{Q_R(T)}\exp\left(-\frac{\Delta E^{\ddagger}}{RT}\right), \qquad (1)$$

where R is the universal constant of the ideal gas, k_B is the Boltzmann constant, h is Planck's constant, $Q^{\ddagger}(T)$ and $Q_R(T)$ are the partition functions of the TS and reactant, respectively, $\Delta E^{\ddagger}$ is the potential energy

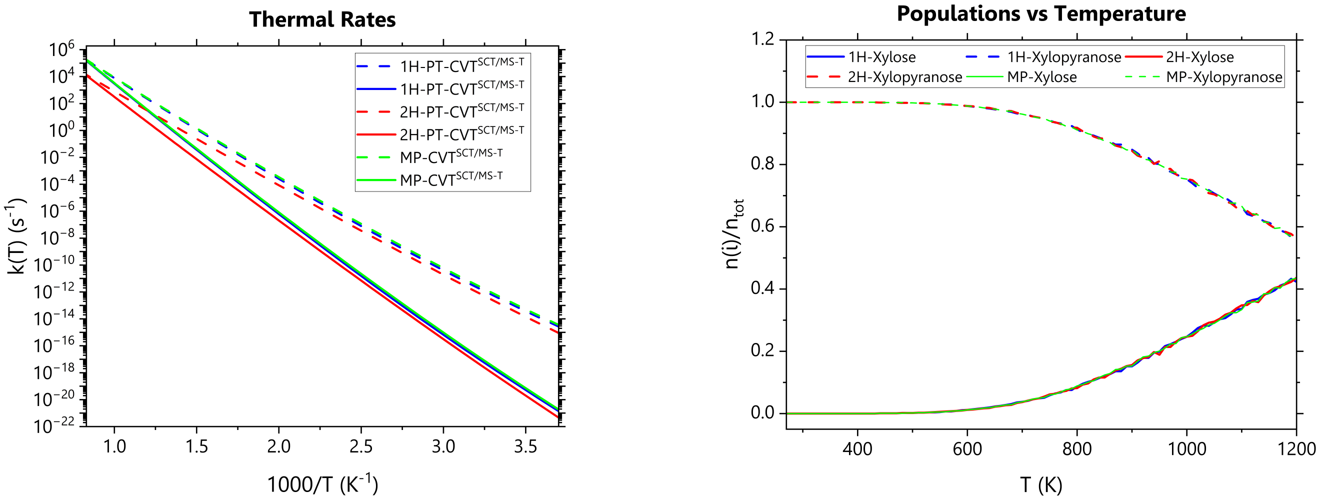

FIGURE 2 The left panel depicts the forward (solid lines) and backward (dash lines) rates for the single (blue) and double (red) proton transfers, along with the multi-path (MP) corrections (green lines). In the right panel, a kinetic Monte-Carlo simulation shows that the relative population of reactant (xylopyranose) and product (xylose) does not change for either mechanism. CVT is the canonical variational transition state theory, SCT stands for semiclassical small-curvature tunneling approximation, and MS-T corresponds to the multi-structural torsional method.

TABLE 1 Fitted Arrhenius parameters over the 270-1200 K temperature interval. The forward/backward reaction values and their corresponding root mean square errors (RMSE) are reported in each entry.

	MP-CVT$^{SCT/MS-T}$	1H-PT-CVT$^{SCT/MS-T}$	2H-PT-CVT$^{SCT/MS-T}$
A /s^{-1}	$3.16 \times 10^{13}/5.28 \times 10^{11}$	$3.58 \times 10^{13}/6.92 \times 10^{11}$	$7.82 \times 10^{11}/1.28 \times 10^{10}$
E_a /kcal mol^{-1}	45.7/35.7	46.2/36.5	43.0/33.0
RMSE	223.39/57.66	179.75/450.31	3.14/5.49

barrier height, and $\kappa(T)$ is the transmission coefficient that accounts for quantum tunneling effects.

In VTST, the location of the dividing surface is varied to minimize the rate constant, leading to the canonical variational transition state theory (CVT) expression:

$$k_{\mathrm{CVT}}(T) = \min_{s} \left\{ \kappa(T,s) \frac{k_B T}{h} \frac{Q^{\ddagger}(T,s)}{Q_R(T)} \exp\left(-\frac{V(s)}{RT}\right) \right\}, \tag{2}$$

where the reaction coordinate s is varied to find the minimum value of the rate constant, $V(s)$ is the potential energy, and $\kappa(T,s)$ is the temperature-dependent transmission coefficient.

In reactions with multiple possible transition states or pathways, MP-VTST provides a more accurate estimation of the overall reaction rate by summing the contributions of each pathway, weighted by their individual rate constants.

The overall rate constant $k_{\text{MP-CVT}}$ is given by:

$$k_{\text{MP-CVT}}(T) = \sum_j k_j(T) \tag{3}$$

where $k_j(T)$ is the rate constant of the j-th reaction path.

Quantum mechanical tunneling effects have been considered by using small curvature tunneling (SCT) corrections. The transmission coefficient κ_j of each path is given by:

$$\kappa_j = \exp\left(-\frac{2}{\hbar}\int_{s_1}^{s_2} \left[2\mu\left(V(s)-E\right)\right]^{1/2} ds\right) \tag{4}$$

where μ is the reduced mass along the reaction coordinate, s_1 and s_2 are the turning points of the reaction coordinate where $V(s) = E$.

By summing the rate constants for all significant pathways, MP-VTST provides a comprehensive rate constant that accounts for the contributions of multiple reaction mechanisms, each characterized by its own TS and PES. This method is particularly useful for complex reactions with competing pathways, ensuring a more accurate prediction of the overall reaction kinetics.

Torsional anharmonicity, arising from the non-rigid nature of molecular torsional modes, can significantly affect the partition functions and, consequently, the rate constants. For each mode, the torsional anharmonic partition function, Q_{tor}, is computed using the `MSTor` program:

$$Q_{\text{tor}} = \int_0^{2\pi} \exp\left(-\frac{V(\phi)}{k_B T}\right) d\phi, \tag{5}$$

where $V(\phi)$ is the potential energy as a function of the torsional angle ϕ. See the SI for detailed analyses of anharmonicity, tunneling, recrossing coefficients, and a comparison of transition state theories.

The kinetic results unveil that the single proton transfer rate exceeds that of the new TS in both the forward and backward directions across the temperature range. In particular, the rate ratio of the ring-opening process ranges from five to eight within the pyrolysis regime, 673.15-873.15 K. Additionally, at any given temperature, both mechanisms are kinetically faster in the backward direction, highlighting their thermally driven nature (see Fig. 2, left panel). For single and double proton migrations, kinetic Monte-Carlo simulations show that the xylopyranose-to-xylose thermal conversion becomes significant near the upper limit of the pyrolysis interval (see Fig. 2, right panel). The Arrhenius parameters derived from fitting the forward rates of the single proton channel align closely with recent reports Lupi et al. (2024), Ayarde-Henríquez et al. (2024), as presented in Table 1. A quantitative analysis of both mechanisms' thermal rates across a pyrolysis-relevant temperature range is provided in the SI.

In conclusion, the new transition state converting β-D-xylopyranose into D-xylose features a synchronous double proton transfer, contrasting with the well-established single proton mechanism. While this alternative channel is energetically favorable by 1.5 kcal mol^{-1}, it is kinetically slower in the pyrolysis regime (673.15-873.15 K) by a factor of 5-8. However, this finding underscores the double proton transfers' relevance in chemistry and biology, as similar reactions might occur in hemicellulose motifs, potentially influencing the kinetics.

ACKNOWLEDGMENTS

This publication has emanated from research conducted with philanthropic financial support of the Ryanair Sustainable Aviation Research Centre at Trinity College Dublin, the European Union through the European Research Council, Mod-L-T, action number 101002649, and the Science Foundation Ireland (SFI) under grant number 12/RC/2278_2. This publication is also cofunded under the European Regional Development Fund under the AMBER award. The authors wish to acknowledge the Irish Centre for High-End Computing (ICHEC) and Luxembourg national supercomputer MeluXina for the provision of computational facilities and support.

CONFLICT OF INTEREST

The authors declare no potential conflict of interests.

REFERENCES

Ayarde-Henríquez, L., Lupi, J. & Dooley, S. (2024) Hemicellulose pyrolysis: mechanism and kinetics of functionalized xylopyranose. *Phys. Chem. Chem. Phys.*, 26(16), 12820–12837.

Ballotta, B., Lupi, J., Ayarde-Henríquez, L. & Dooley, S. (2024) Ab initio conformational analysis of α/β-d-xylopyranose at pyrolysis conditions. *Phys. Chem. Chem. Phys.*, 26(47), 29661–29673.

Chen, W., Zheng, J., Bao, J.L., Truhlar, D.G. & Xu, X. (2023) Mstor 2023: A new version of the computer code for multistructural torsional anharmonicity, now with automatic torsional identification using redundant internal coordinates. *Comput. Phys. Commun.*, 288, 108740.

Ferro-Costas, D., Truhlar, D.G. & Fernández-Ramos, A. (2020) Pilgrim: A thermal rate constant calculator and a chemical kinetics simulator. *Comput. Phys. Commun.*, 256, 107457.

Frisch, M.J., Trucks, G.W., Schlegel, H.B., Scuseria, G.E., Robb, M.A., Cheeseman, J.R. et al. (2016) *Gaussian16 Revision C.01*. Gaussian Inc. Wallingford CT.

Fukui, K. (1981) The path of chemical reactions - the irc approach. *Acc. Chem. Res.*, 14(12), 363–368.

Garay-Ruiz, D., Álvarez Moreno, M., Bo, C. & Martínez-Núñez, E. (2022) New tools for taming complex reaction networks: The unimolecular decomposition of indole revisited. *ACS Phys. Chem Au*, 2(3), 225–236. doi:10.1021/acsphyschemau.1c00051.

Grimme, S., Ehrlich, S. & Goerigk, L. (2011) Effect of the damping function in dispersion corrected density functional theory. *J. Comput. Chem.*, 32(7), 1456–1465.

Hu, B., Lu, Q., Zhang, Z.X., Wu, Y.T., Li, K., Dong, C.Q. et al. (2019) Mechanism insight into the fast pyrolysis of xylose, xylobiose and xylan by combined theoretical and experimental approaches. *Combust. Flame*, 206, 177–188.

Kozuch, S. & Martin, J.M.L. (2011) DSD-PBEP86: in search of the best double-hybrid DFT with spin-component scaled MP2 and dispersion corrections. *Phys. Chem. Chem. Phys.*, 13, 20104–20107.

Lupi, J., Ayarde-Henríquez, L., Kelly, M. & Dooley, S. (2024) Ab initio and kinetic modeling of β-d-xylopyranose under fast pyrolysis conditions. *J. Phys. Chem. A*, 128(6), 1009–1024.

Martínez-Núñez, E. (2015) An automated method to find transition states using chemical dynamics simulations. *J. Comput. Chem.*, 36(4), 222–234.

Martínez-Núñez, E. (2015) An automated transition state search using classical trajectories initialized at multiple minima. *Phys. Chem. Chem. Phys.*, 17, 14912–14921.

Martínez-Núñez, E., Barnes, G.L., Glowacki, D.R., Kopec, S., Peláez, D., Rodríguez, A. et al. (2021) Automekin2021: An open-source program for automated reaction discovery. *J. Comput. Chem.*, 42(28), 2036–2048.

Neese, F. (2022) Software update: The orca program system—version 5.0. *Wiley Interdiscip. Rev. Comput. Mol. Sci.*, 12(5), e1606.

Papajak, E., Zheng, J., Xu, X., Leverentz, H.R. & Truhlar, D.G. (2011) Perspectives on basis sets beautiful: Seasonal plantings of diffuse basis functions. *J. Chem. Theory Comput.*, 7, 3027–3034.

Peterson, K.A. & Dunning, T.H. (2002) Accurate correlation consistent basis sets for molecular core-valence correlation effects: The second row atoms al-ar, and the first row atoms b-ne revisited. *J. Chem. Phys.*, 117, 10548–10560. doi:10.1063/1.1520138.

Riplinger, C., Sandhoefer, B., Hansen, A. & Neese, F. (2013) Natural triple excitations in local coupled cluster calculations with pair natural orbitals. *J. Chem. Phys.*, 139(13), 134101.

Stewart, J.J.P. (2013) Optimization of parameters for semiempirical methods vi: more modifications to the nddo approximations and re-optimization of parameters. *J. Mol. Model.*„ 1–32.doi:https://doi.org/10.1007/s00894-012-1667-x.

Stewart, J.J.P. (2016) Mopac2016,.
URL HTTP://OpenMOPAC.net

SUPPORTING INFORMATION

Additional supporting information may be found in the online version of the article at the publisher's website.